Inorganic Chemistry

Article

pubs.acs.org/IC

Kinetic and Mechanistic Aspects of Atom Transfer Radical Addition (ATRA) Catalyzed by Copper Complexes with Tris(2-pyridylmethyl)amine

William T. Eckenhoff, Ashley B. Biernesser, and Tomislav Pintauer*

Department of Chemistry and Biochemistry, Duquesne University, 600 Forbes Avenue, 308 Mellon Hall, Pittsburgh, Pennsylvania 15282, United States

Supporting Information

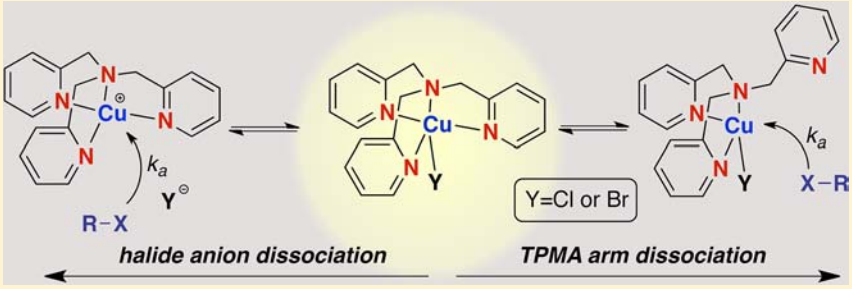

ABSTRACT: Kinetic and mechanistic studies of atom transfer radical addition (ATRA) catalyzed by copper complexes with tris(2-pyridylmethyl)amine (TPMA) ligand were reported. In solution, the halide anions were found to strongly coordinate to $[Cu^{I}(TPMA)]^{+}$ cations, as confirmed by kinetic, cyclic voltammetry, and conductivity measurements. The equilibrium constant for atom transfer ($K_{ATRA} = k_a/k_d$) utilizing benzyl thiocyanate was determined to be approximately 6 times larger for $Cu^{I}(TPMA)BPh_4$ ($(1.6 \pm 0.2) \times 10^{-7}$) than $Cu^{I}(TPMA)Cl$ ($(2.8 \pm 0.2) \times 10^{-8}$) complex. This difference in reactivity between $Cu^{I}(TPMA)Cl$ and $Cu^{I}(TPMA)BPh_4$ was reflected in the activation rate constants ($(3.4 \pm 0.4) \times 10^{-4}$ M^{-1} s^{-1} and $(2.2 \pm 0.2) \times 10^{-3}$ M^{-1} s^{-1}, respectively). The fluxionality of $Cu^{I}(TPMA)X$ (X = Cl or Br) in solution was mainly the result of TPMA ligand exchange, which for the bromide complex was found to be very fast at ambient temperature ($\Delta H^{\ddagger} = 29.7$ kJ mol^{-1}, $\Delta S^{\ddagger} = -60.0$ J K^{-1} mol^{-1}, $\Delta G^{\ddagger}_{298} = 47.6$ kJ mol^{-1}, and $k_{obs,298} = 2.9 \times 10^4$ s^{-1}). Relatively strong coordination of halide anions in $Cu^{I}(TPMA)X$ prompted the possibility of activation in ATRA through partial TPMA dissociation. Indeed, no visible differences in the ATRA activity of $Cu^{I}(TPMA)BPh_4$ were observed in the presence of as many as 5 equiv of strongly coordinating triphenylphosphine. The possibility for arm dissociation in $Cu^{I}(TPMA)X$ was further confirmed by synthesizing tris(2-(dimethylamino)phenyl)amine (TDAPA), a ligand that was structurally similar to currently most active TPMA and Me_6TREN (tris(2-dimethylaminoethyl)-amine), but had limited arm mobility due to the rigid backbone. Indeed, $Cu^{I}(TDAPA)Cl$ complex was found to be inactive in ATRA, and the activity increased only by opening the coordination site around the copper(I) center by replacing chloride anion with less coordinating counterions such as BF_4^- and BPh_4^-. The results presented in this Article are significant from the mechanistic point of view because they indicate that coordinatively saturated $Cu^{I}(TPMA)X$ complexes catalyze the homolytic cleavage of carbon−halogen bond during the activation step in ATRA by prior dissociation of either halide anion or TPMA arm.

INTRODUCTION AND BACKGROUND

Atom transfer radical addition (ATRA) is a facile technique for the formation of carbon−carbon bonds utilizing alkyl halides and alkenes. The reaction originates from the Kharasch addition,[1,2] and it is typically catalyzed by transition metal complexes of copper or ruthenium.[3−12] Traditionally, ATRA required rather large amounts of metal catalyst to achieve high chemoselectivity toward the desired single addition adduct. However, the use of reducing agents such as free radicals generated by thermal or photodecomposition of diazo initiators (2,2′-azobis(2-methylpropionitrile) (AIBN)[13−27] and 2,2′-azobis(4-methoxy-2,4-dimethyl valeronitrile) (V-70)[28]), magnesium,[29−36] or environmentally benign ascorbic acid[24,37] successfully circumvented this problem. As a result, this organic transformation can now be conducted using very low amounts of the metal.[20,38−40] ATRA has long been accepted to involve free radical intermediates.[10,41] Shown in Scheme 1 is the proposed mechanism for copper catalyzed ATRA in the presence of reducing agents. The catalytic cycle starts with a reduction of copper(II) (deactivator) to the corresponding copper(I) complex (activator). In the next step, homolytic cleavage of an alkyl halide bond by the copper(I) complex generates a primary organic radical that adds across the carbon−carbon double bond of an alkene. The secondary radical then irreversibly abstracts halogen atom from the

Received: August 20, 2012
Published: October 10, 2012

   dx.doi.org/10.1021/ic3018198 | Inorg. Chem. 2012, 51, 11917−11929

Scheme 1. Proposed Mechanism for Copper Catalyzed Atom Transfer Radical Addition (ATRA) in the Presence of Reducing Agents

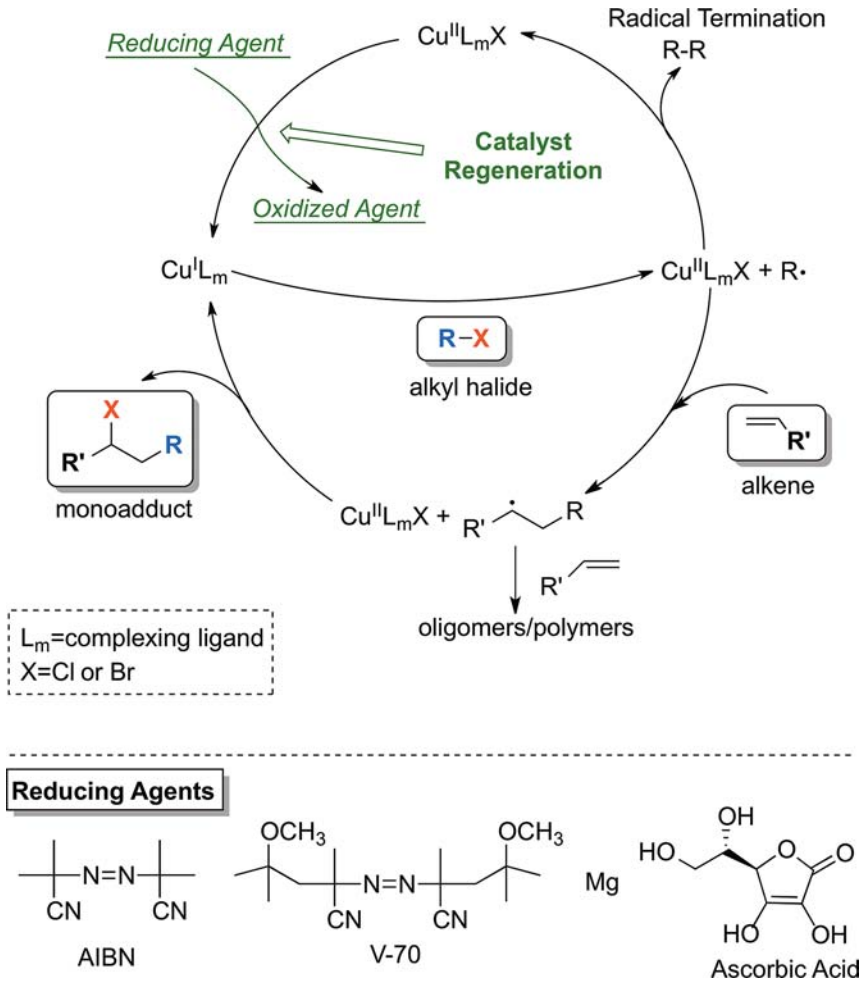

copper(II) complex to form the desired monoadduct. This last step also regenerates the copper(I) complex and therefore completes the catalytic cycle.

As indicated in Scheme 1, concurrent side reactions that compete with monoadduct formation include oligomerization/polymerization and radical–radical termination by either coupling or disproportionation. Although oligomerization/polymerization reactions can be suppressed by the appropriate selection of the catalyst, alkene, and alkyl halide, termination reactions cannot be avoided because they are typically diffusion controlled ($k_t \approx 2.0 \times 10^9$ M^{-1} s^{-1}).[42] Every termination step in ATRA results in accumulation of the deactivator species or copper(II) complex.[40,43] In order to compensate for this unwanted side reaction, reducing agents are introduced into the reaction mixture to continuously regenerate the activator or copper(I) complex. The advantages of this new methodology are 2-fold. On one hand, reducing agents enable a significant reduction in the amount of copper catalyst, and on the other, ATRA reactions can be conducted starting with the air stable copper(II) complexes which surpasses otherwise necessary deoxygenation techniques.[20]

The activation step in copper catalyzed ATRA is widely accepted to proceed via an inner-sphere electron transfer (ISET).[44−47] The ISET process requires the alkyl halide to come within the bonding distance of the copper(I) complex, where the halide forms pseudobonds with both the alkyl group and metal center. Following the electron transfer, this bond is then homolytically cleaved, generating the copper(II) complex and alkyl radical (Scheme 2).[48] Currently, one of the most

Scheme 2. ISET and OSET Processes During Activation Step in Copper Catalyzed ATRA (Adopted from Reference 48)

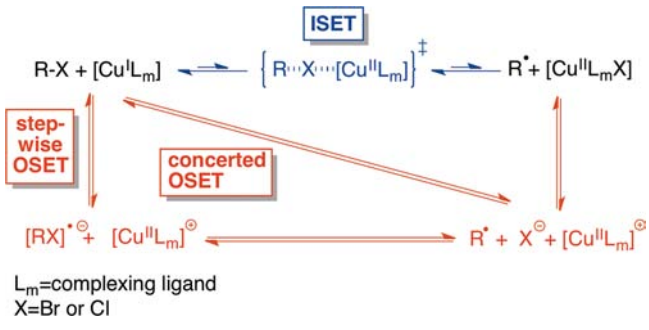

highly active copper catalysts for this transformation is Cu^{I}(TPMA)X (X = Cl or Br, TPMA = tris(2-pyridylmethyl)-amine). These complexes were found to be pseudopentacoordinated in the solid state because of the chelation from both tetradentate TPMA ligand and halide anion.[15,16,49] When the structure was probed in solution, Cu^{I}(TPMA)X complexes

dx.doi.org/10.1021/ic3018198 | Inorg. Chem. 2012, 51, 11917−11929

were observed to be fluxional at room temperature. However, they retained C_3 symmetry indicating that all three arms of TPMA were symmetrically coordinated to the copper(I) center. In the absence of halide anions or other monodentate ligands (CH_3CN or PPh_3), copper(I) complexes dimerized in an unsymmetrical manner, giving rise to a distinctive NMR spectra as a result of inequivalent methylene protons in TPMA.[50] The possibility of halide anion coordination in solution was surprising because such complex would formally be described as coordinatively saturated. In such a case, a dissociation of the ligand arm must occur for an ISET process, raising the possibility that the activation step might occur via an outer sphere electron transfer (OSET). The OSET mechanism can be described as proceeding via concerted or stepwise pathways (Scheme 2). In the concerted pathway, dissociative electron transfer oxidizes the copper(I) complex and reduces the alkyl halide to an alkyl radical and halide anion. On the other hand, the stepwise pathway first involves the formation of a radical anion on the alkyl halide after oxidation of the copper(I) complex, subsequently followed by cleavage into radical and halide anion. In both cases, the halide eventually associates with the copper(II) complex.

Recently, extensive *ab initio* calculations probed the mechanism of each process in order to determine the activation enthalpies in the gas phase and solution (DMF and CH_3CN).[48] For the model system consisting of a copper(I) complex with TPMA ligand and ethyl-2-bromoisobutyrate as the alkyl halide, the adiabatic reduction of RX to $RX^{\bullet-}$ (the first step of the stepwise OSET pathway, Scheme 2) was calculated to be endoergic by 20.3 kcal mol^{-1} in acetonitrile at 25 °C. This was substantially higher than the values for both ISET and concerted OSET mechanisms. On a thermodynamic basis, the latter two pathways could not be distinguished because they gave the same final products. However, Marcus theory of electron transfer, coupled with experimentally measured reduction potentials for $Cu^{I/II}$/TPMA and alkyl halide, as well as bond dissociation energy for carbon halogen bond, was used to approximate the rate constant for OSET. Using the same copper catalyst and bromoacetonitrile in CH_3CN at 25 °C, the estimated rate constant $k_{OSET} \approx 10^{-11}$ M^{-1} s^{-1} was significantly smaller than the experimentally measured activation rate constant $k_{ISET} \approx 10^{2}$ $M^{-1}s^{-1}$ for the concerted atom transfer mechanism or ISET, implying that the ISET pathway was strongly preferred. In conjunction with these, along with results obtained in our laboratories, additional studies into the catalytic mechanism of alkyl halide cleavage by Cu^{I}(TPMA)X complexes are warranted.

In this Article, we report on further kinetic and mechanistic studies of atom transfer radical addition (ATRA) catalyzed by copper complexes with tris(2-pyridylmethyl)amine (TPMA) ligand. More precisely, the effects of counterion, auxiliary monodentate ligands such as PPh_3, and halide anion/TPMA dissociation will be examined.

EXPERIMENTAL SECTION

General Procedures. All chemicals were purchased from commercial sources and used as received. Tris(2-pyridylmethyl)amine (TPMA),[51] tris(2-(dimethylamino)phenyl)amine (TDAPA),[52] tetrakis(acetonitrile)copper(I) perchlorate,[53] Cu^{I}(TPMA)X (X = Br^-, Cl^-, ClO_4^-, PF_6^- and BPh_4^-),[15,16,50] and $[Cu^{I}(TPMA)PPh_3]$-$[BPh_4]$[50] were synthesized according to previously published literature procedures. Although we experienced no problems, perchlorate metal salts are potentially explosive and should be handled with care. All manipulations involving copper(I) complexes were performed under argon in the drybox (<1.0 ppm O_2 and <0.5 ppm H_2O) or using standard Schlenk line techniques. Solvents (pentane, acetonitrile, acetone, and diethyl ether) were degassed and deoxygenated using an Innovative Technology solvent purifier. Methanol was vacuum distilled and deoxygenated by bubbling argon for 30 min prior to use. Copper(II) complexes were synthesized under ambient conditions, and solvents were used as received.

Instrumentation and Equipment. ^{1}H NMR spectra were obtained using Bruker Avance 400 and 500 MHz spectrometers, and chemical shifts are given in ppm relative to residual solvent peaks [$CDCl_3$ δ7.26 ppm; $(CD_3)CO$ δ2.05 ppm; CD_3CN δ1.96 ppm]. iNMR and KaleidaGraph 4.1 software were used to generate images of NMR spectra. Temperature calibrations were performed using a pure methanol sample. Conductivity measurements were performed using a VWR Traceable Bench/Portable Conductivity Meter (23226−505) in a drybox (O_2 < 0.5 ppm) using 1 mM solutions of copper complexes in acetonitrile. IR spectra were recorded in the solid state using Nicolet Smart Orbit 380 FT-IR spectrometer (Thermo Electron Corporation). Elemental analyses for C, H, and N were obtained from Midwest Microlabs, LLC. UV−vis spectra were recorded using a Beckman DU-530 spectrometer in 1.0 cm path-length airtight quartz cuvettes. Electrochemical measurements were carried out using Bioanalytical Systems (BAS) model CV-50W in a drybox. Cyclic voltammograms were recorded with a standard three-electrode system consisting of a Pt-wire working electrode, a standard calomel reference electrode, and a Pt-wire auxiliary electrode. Tetrabutylammonium perchlorate (TBA-ClO_4), tetrabutylammonium tetraphenylborate (TBA-BPh_4), tetrabutylammonium chloride (TBA-Cl), and tetrabutylammonium bromide (TBA-Br) were used as the supporting electrolytes, and all voltammograms were externally referenced to ferrocene. As such, the potentials are reported with respect to Fc/Fc^+ couple, without junction correction. All cyclic voltammograms were simulated digitally to obtain the half-wave potentials.

X-ray Crystal Structure Determination. The X-ray intensity data were collected at 150 K using graphite-monochromated Mo K radiation (0.710 73 Å) with a Bruker Smart Apex II CCD diffractometer. Data reduction included absorption corrections by the multiscan method using SADABS.[54] Structures were solved by direct methods and refined by full matrix least-squares using SHELXTL 6.1 bundled software package.[55] The H-atoms were positioned geometrically (aromatic C−H 0.93, methylene C−H 0.97, and methyl C−H 0.96) and treated as riding atoms during subsequent refinement, with $U_{iso}(H) = 1.2U_{eq}(C)$ or $1.5U_{eq}$(methyl C). The methyl groups were allowed to rotate about their local 3-fold axes. ORTEP-3 for Windows[56] and Crystal Maker 8.3 were used to generate molecular graphics. For detailed crystallographic data tables refer to Supporting Information.

General Procedure for Copper Catalyzed ATRA in the Presence of AIBN. In a glass vial, alkene (3.22 mmol), CCl_4 (310 μL, 3.22 mmol), and AIBN (26.4 mmol, 0.160 mmol) were combined, followed by the addition of CH_3CN (1.22 mL for 1-hexene or 1-octene and 0.896 mL for styrene or methyl acrylate). 1,4-Dimethoxybenzene was added as an internal standard. The reaction mixture was then divided equally into four disposable NMR tubes (5 mm), and different amounts of copper(II) complex from a 0.0100 M solution in CH_3CN were added. The initial concentration of alkene in each NMR tube was maintained at 2.10 M by the addition of appropriate amount of CH_3CN (total volume = 384 μL). The tubes were then flushed with argon for 30 s, capped with a standard plastic NMR tube cap, sealed with a Teflon tape, and finally placed in an oil bath thermostatted at 60 °C. After 24 h, the conversion of alkene and the yield of monoadduct were determined using ^{1}H NMR spectroscopy.

General Procedure for Copper Catalyzed ATRA in the Absence of AIBN. In a drybox (O_2 < 1.0 ppm), methyl acrylate (580 μL, 6.44 mmol) was combined with CCl_4 (622 μL, 6.44 mmol), 0.0644 mmol of copper(I), and 6.44 × 10^{-3} mmol of copper(II) complex. 1,4-Dimethoxybenzene was added as an internal standard, followed by further dilution with CH_3CN (1.87 mL) in order to maintain the initial alkene concentration at 2.10 M. The reaction

dx.doi.org/10.1021/ic3018198 | Inorg. Chem. 2012, 51, 11917−11929

mixture was then divided equally into eight disposable NMR tubes (5 mm), which were capped with a standard plastic NMR tube cap, sealed with a Teflon tape, and finally placed in an oil bath thermostatted at 60 °C. Each NMR tube was removed at timed intervals and the conversion of alkene and the yield of monoadduct determined using ^{1}H NMR spectroscopy.

Triphenylphosphine Inhibition Reactions. In a glass vial, alkene (4.03 mmol) was added to a solution containing CCl_4 (388 μL, 4.03 mmol), AIBN (33.1 mg, 0.200 mmol), and [Cu^{II}(TPMA)Cl][Y] (Y = Cl^- or BPh_4^-) complex (8.00×10^{-4} mmol, 80.0 μL from 0.0100 M solution in CH_3CN). The total volume was adjusted to 1.18 mL by the addition of CH_3CN and 1,4-dimethoxybenzene added as an internal standard. The reaction mixture was then divided equally into five disposable NMR tubes (5 mm), and different amounts of triphenylphosphine were added (from a 0.0500 M solution in CH_3CN). The initial concentration of alkene in each NMR tube was maintained at 2.40 M by the addition of the appropriate amount of CH_3CN. The tubes were then flushed with argon for 30 s, capped with a standard plastic NMR tube cap, sealed with a Teflon tape, and finally placed in an oil bath thermostatted at 60 °C. After 24 h, the conversion of alkene and the yield of monoadduct were determined using ^{1}H NMR spectroscopy.

Thermodynamic Parameters for TPMA Exchange. In a drybox (O_2 < 1.0 ppm), Cu^I(TPMA)Br (20.0 mg, 4.61×10^{-2} mmol) and 1.0 equiv of TPMA (13.4 mg, 4.61×10^{-2} mmol) were dissolved in acetone-d_6 and placed in an airtight 5 mm J. Young NMR tube. Variable temperature ^{1}H NMR spectra were then collected between 298 and 170 K. The rate constant for exchange between free and coordinated TPMA ligand was calculated at each temperature according to previously reported procedures.[57] Thermodynamic parameters ($\Delta H^{\ddagger}$ and $\Delta S^{\ddagger}$) were determined using the Eyring equation.

Determination of the Equilibrium Constant for Atom Transfer (K_{ATRA}). Cu^I(TPMA)X (X = Cl^- or BPh_4^-) (2.50×10^{-2} mmol) and benzyl thiocyanate (37.3 mg, 0.250 mmol) were dissolved in 5.00 mL of acetonitrile. An aliquot was quickly transferred to an airtight cuvette and removed from the drybox. The absorbance of the copper(II) complex was monitored by UV−vis spectroscopy at λ_{max} (952 nm for [Cu^{II}(TPMA)NCS][Cl] and 891 nm for [Cu^{II}(TPMA)-NCS][BPh_4]) for 6 h. The equilibrium constant for atom transfer (K_{ATRA}) was calculated using previously published procedures (see Supporting Information).[58−60]

Determination of the Activation Rate Constants (k_a). Cu^I(TPMA)X (X = Cl^- or BPh_4^-) (2.50×10^{-2} mmol) and TEMPO (2,2,6,6-tetramethyl-1-piperidinyloxy) (78.1 mg, 0.500 mmol) were dissolved in 5.00 mL of acetonitrile. Following the addition of benzyl thiocyanate (74.6 mg, 0.500 mmol), an aliquot was quickly transferred to an airtight cuvette and removed from the drybox. The absorbance of the copper(II) complex was monitored by UV−vis spectroscopy at λ_{max} (952 nm for [Cu^{II}(TPMA)NCS][Cl] and 891 nm for [Cu^{II}(TPMA)NCS][BPh_4]) for 6 h. The activation rate constant (k_a) was determined from first order kinetic plots as reported in the literature (see Supporting Information).[60,61]

Synthesis of Benzyl Thiocyanate. Benzyl bromide (1.21 g, 7.07 mmol) and sodium thiocyanate (0.860 g, 10.6 mmol) were added to 50 mL of water/acetone solution (4:1 vol %) in a Schlenk flask and heated at 80 °C for 8 h. After the completion, the layers were separated, and the aqueous layer was further extracted with diethyl ether (3 × 10 mL). The organic fractions were combined, dried over $MgSO_4$, and evaporated to give a white solid. The crude product was further purified by sublimation to yield 0.792 g of benzyl thiocyanate (76%). ^{1}H NMR (400 MHz, $CDCl_3$, 298 K): δ 7.43−7.36 (m, 5H), 4.16 (s, 2H). ^{13}C NMR (101 MHz; $CDCl_3$, 298 K): δ134.4, 129.2, 129.0, 128.9, 112.1, 38.4. FT-IR (solid): ν(cm^{-1}) = 3033(w), 2988(w), 2144(s), 1489(m), 1455(m) 1422(m), 1244(m), 766(m), 700(m), 644(m).

Synthesis of [Cu^I(TDAPA)(CH_3CN)][ClO_4]. Tris(2-(dimethylamino)phenyl)amine (TDAPA) (50.0 mg, 0.130 mmol) was dissolved in 5.0 mL of acetonitrile and 44.0 mg (0.130 mmol) of [$Cu^I(CH_3CN)_4$][ClO_4] added. The mixture was stirred at ambient temperature until all materials dissolved. Following the addition of 10.0 mL of diethyl ether, the solution was placed in the freezer at −35 °C overnight. The white powder was collected by filtration to yield 40.2 mg (52%) of [Cu^I(TDAPA)(CH_3CN)][ClO_4]. Slow evaporation of diethyl ether into a concentrated acetonitrile solution of the complex afforded colorless crystals suitable for X-ray analysis. ^{1}H NMR ($(CD_3)_2CO$, 400 MHz, 296 K): δ 7.49−7.22 (m, 12H), 3.13 (bs, 3H), 2.28 (s, 18H). Anal. Calcd for $C_{26}H_{33}ClCuN_5O_4$ (578.56): C, 53.97; H, 5.75; N, 12.10. Found: C, 53.75; H, 5.66; N, 12.03.

Synthesis of [Cu^{II}(TPMA)NCS][BPh_4]. Previously synthesized [Cu^{II}(TPMA)Cl][BPh_4][50] (0.448 g, 0.63 mmol) was dissolved in 20 mL of methylene chloride and sodium thiocyanate (0.051 g, 0.63 mmol) added. Solution was allowed to stir at ambient temperature for 1 h and filtered to remove sodium chloride. The green product was precipitated by the addition of 50 mL of pentane and dried under vacuum to yield [Cu^{II}(TPMA)NCS)][BPh_4] (0.226 g, 49%). UV−vis (CH_3CN): λ_{max} = 891 nm, ε_{max} = 266 L mol^{-1} cm^{-1}. FT-IR (solid): ν(cm^{-1}) = 3059(w), 2986(w), 2925(w), 2090(s), 1605(m), 1476(m), 1433(m), 1032(w), 703(m). Anal. Calcd for $C_{43}H_{38}N_5CuBS$ (731.22): C, 70.63; H, 5.24; N, 9.58. Found: C, 70.78; H, 5.32; N, 9.62.

Synthesis of [Cu^{II}(TPMA)NCS][Cl]. Previously synthesized [Cu^{II}(TPMA)Cl][Cl][16] (0.200 g, 0.470 mmol) was dissolved in 5 mL of methylene chloride and sodium thiocyanate (0.038 g, 0.470 mmol) added. Solution was allowed to stir at ambient temperature for 1 h and filtered to remove sodium chloride. The green product was precipitated by the addition of 30 mL of pentane and dried under vacuum to yield [Cu^{II}(TPMA)NCS][Cl] (0.154 g, 73%). UV−vis (CH_3CN): λ_{max} = 952 nm, ε_{max} = 212 L mol^{-1} cm^{-1}. FT-IR (solid): ν(cm^{-1}) = 3066(w), 2907(w), 2050(s), 1606(s), 1433(m), 1303(w), 1021(m), 764(m). Anal. Calcd for $C_{19}H_{18}N_5CuClS$ (447.44): C, 51.00; H, 4.05; N, 15.65. Found: C, 50.85; H, 4.06; N, 15.71.

RESULTS AND DISCUSSION

Effect of Counterion on ATRA Catalyzed by [Cu^{II}(TPMA)Cl[Y] (Y = Cl^-, PF_6^-, ClO_4^-, and BPh_4^-) Complexes. The counterion in copper(I) complexes with TPMA ligand drastically influences not only the electrochemistry,[15] but also the molecular structure in the solid state and solution.[50] Since it has been shown that redox potential directly correlates with the equilibrium constant for atom transfer (ratio of activation to deactivation rate constants, $K_{ATRA} = k_a/k_d$),[43,62] we anticipated that much less reducing copper(I) complexes with ClO_4^-, PF_6^-, and BPh_4^- anions would show lower activity in ATRA than the corresponding Br^- and Cl^- analogues.[15,16] The results for the ATRA of CCl_4 to 1-hexene, 1-octene, styrene, and methyl acrylate catalyzed by [Cu^{II}(TPMA)Cl][Y] (Y = ClO_4^-, PF_6^-, and BPh_4^-) in the presence of AIBN are summarized in Table 1. The results clearly indicate that in the presence of AIBN no differences in alkene conversion and monoadduct yield were observed after 24 h. Regardless of the solvent, for 1-hexene and 1-octene nearly quantitative yields of the monoadduct were achieved using as low as 0.02 mol % of the copper catalyst (relative to alkene). In the case of styrene and methyl acrylate, the yields of approximately 65% were observed at a 500:1 ratio (0.20 mol %), which was consistent with our previous studies utilizing Cu^I(TPMA)Cl and [Cu^{II}(TPMA)Cl][Cl] complexes.[16] The only noticeable difference was observed in the case of the addition of CCl_4 to styrene, which showed a slight decrease in conversion in acetonitrile when compared to methanol. This can be attributed to a lower reducing power of copper(I) complexes in acetonitrile due to solvent coordination, as observed previously.[50,63,64]

Our research group has shown that the rate of alkene consumption in copper catalyzed ATRA in the presence of reducing agents is rather complicated.[14,21,23] When free radicals

Table 1. ATRA Reactions of CCl_4 to Different Alkenes Catalyzed by $[Cu^{II}(TPMA)Cl][Y]$ (Y = Cl^-, ClO_4^-, PF_6^-, and BPh_4^-) Complexes in the Presence of AIBN[a]

$[Y]^-$	alkene	$[Cu^{II}]$ (mol %)[b]	conv (%)/yield (%)[c] CH_3CN	conv (%)/yield (%)[c] MeOH
Cl	1-hexene	0.02	~100/~100	~100/~100
ClO_4			~100/~100	~100/~100
PF_6			~100/~100	~100/~100
BPh_4			~100/~100	~100/~100[d]
Cl	1-octene	0.02	99/99	99/99
ClO_4			99/99	99/99
PF_6			99/99	99/99
BPh_4			99/99	99/99[d]
Cl	styrene	0.2	85/60	~100/65
ClO_4			85/62	~100/68
PF_6			92/67	~100/67
BPh_4			81/59	~100/72[d]
Cl	methyl acrylate	0.2	~100/62	~100/69
ClO_4			~100/60	~100/73
PF_6			~100/70	~100/76
BPh_4			~100/76	~100/71[d]

[a]Reactions were performed at 60 °C in CH_3CN or CH_3OH, $[alkene]_0/[CCl_4]_0/[AIBN]_0$ = 1/1.1/0.05, $[alkene]_0$ = 2.10 M. [b]mol % relative to alkene. [c]Conversion and yield were determined by ^1H NMR spectroscopy using 1,4-dimethoxybenzene as internal standard (relative errors are ±5.0%). [d]$[Cu(TPMA)Cl][BPh_4]$ was added as a solution in acetone.

generated by thermal decomposition of diazo initiators are used as reducing agents, the rate of disappearance of alkene is governed by the rate of decomposition of the free radical source and not by the concentration or nature of the copper catalyst.[23,65] However, product selectivity was shown to directly correlate with the activity of the catalyst, especially with alkenes that readily polymerize in the presence of free radicals such as styrene, methyl acrylate, or acrylonitrile.[23] Thus, it was not surprising that the observed reaction rates for ATRA in the presence of AIBN with all $[Cu^{II}(TPMA)Cl][Y]$ complexes were nearly identical. Representative first order kinetic plots for 1-octene are shown in Figure 1, with the $k_{obs,av}$ of approximately 2.0×10^{-5} s^{-1}.

In order to eliminate this effect on the reaction kinetics, experiments were performed using larger concentrations of $Cu^I(TPMA)Y$ complexes in the absence of AIBN. Under such reaction conditions, the rate of disappearance of alkene is given by eq 1.

$$-\frac{d[alkene]}{dt} = k_{add}[R^\bullet] \quad (1)$$

Neglecting termination reactions due to persistent radical effect,[58,59,66,67] and using a fast equilibrium approximation, the radical concentration ($[R^\bullet]$) in the system can be calculated using eq 2:

$$Cu^IL_n + RX \underset{k_{d,1}}{\overset{k_{a,1}}{\rightleftarrows}} Cu^{II}L_nX + R^\bullet$$

$$[R^\bullet] = \frac{k_{a,1}[Cu^IL_n][RX]}{k_{d,1}[Cu^{II}L_nX]} \quad (2)$$

Combining these two expressions gives the following rate law for copper catalyzed ATRA gives the following (eq 3):

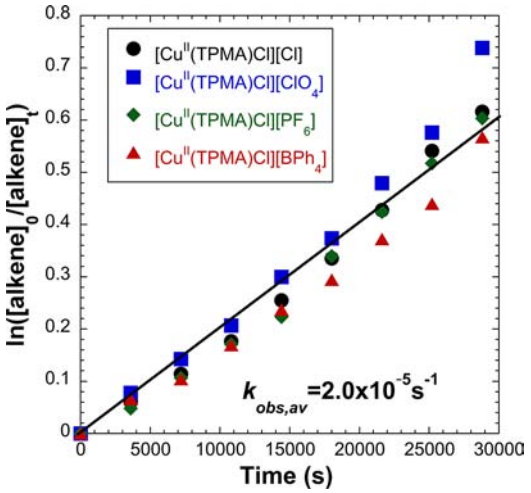

Figure 1. First order kinetic plots for ATRA of CCl_4 to 1-octene catalyzed by $[Cu^{II}(TPMA)Cl][Y]$ complexes in the presence of AIBN, $[alkene]_0/[CCl_4]_0/[AIBN]_0/[Cu^{II}]_0$ = 5000/5000/250/1, $[alkene]_0$ = 2.10 M, solvent = CH_3CN, T = 60 °C.

$$-\frac{d[alkene]}{dt} = \frac{K_{ATRA}k_{add}[Cu^IL_n][RX][alkene]}{[Cu^{II}L_nX]} \quad (3)$$

$$K_{ATRA}^{app} = \frac{K_{ATRA}}{[Cu^{II}L_nX]} = \frac{slope}{k_{add}[Cu^IL_n]_0[RX]_0} \quad (4)$$

Here $K_{ATRA} = k_{a,1}/k_{d,1}$ (subscripts 1 in the rate constants denote the first addition step only). If the radical concentration in the system is constant, a plot of $\ln([alkene]_t/[alkene]_0)$ versus time should give a straight line with the slope being related to the apparent equilibrium constant for atom transfer K_{ATRA}^{app} (eq 4).[13,20,40] Indeed, the corresponding plots for the addition of CCl_4 to methyl acrylate catalyzed by $Cu^I(TPMA)Y$ complexes indicate constant radical concentration in each system (Figure 2). Interestingly, the observed rate constants for copper(I) complexes containing "noncoordinating" anions (k_{obs} = (4.6 ± 0.6) × 10^{-5} s^{-1} ($Cu^I(TPMA)ClO_4$) and (7.6 ± 0.8) × 10^{-5} s^{-1} ($Cu^I(TPMA)BPh_4$)) were found to be higher than for chloride complex (k_{obs} = (1.1 ± 0.2) × 10^{-5} s^{-1}). Similarly, since the

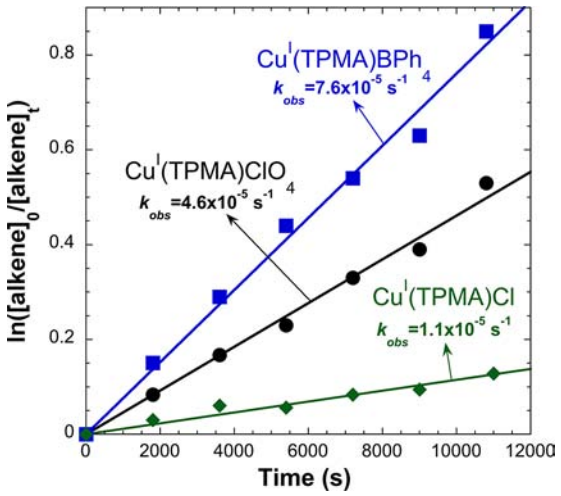

Figure 2. First order kinetics plot for ATRA of CCl_4 to methyl acrylate catalyzed by $Cu^I(TPMA)Y$ complexes, $[alkene]_0/[CCl_4]_0/[Cu]_0$ = 50:50:1, $[alkene]_0$ = 2.10 M, solvent = CH_3CN, T = 60 °C.

dx.doi.org/10.1021/ic3018198 | Inorg. Chem. 2012, 51, 11917−11929

addition rate constant and the initial concentrations of copper(I) and alkyl halide remain constant (eq 4), complexes with perchlorate and tetraphenylborate anions have an apparent equilibrium constant for atom transfer (K_{ATRA}^{app}) approximately 4 and 7 times higher, respectively, than $Cu^{I}(TPMA)Cl$. These results indicate that in the absence of a reducing agent, such as radicals generated from the decomposition of AIBN, ATRA reactions will proceed faster when the coordination sphere of copper(I) complex has an open coordination site and therefore does not require either halide anion or TPMA arm dissociation prior to the activation step ($RX + Cu^{I}L_n \rightarrow Cu^{II}L_nX + R^{\bullet}$). However, this statement needs further validation because the increase in apparent equilibrium constant for atom transfer could alternatively be attributed to a decrease in the deactivation rate constant for the reverse reaction ($Cu^{II}L_nX + R^{\bullet} \rightarrow RX + Cu^{I}L_n$). Hence, we reverted our experiments to independently determine the activation rate constant (k_a) and overall equilibrium constant for atom transfer (K_{ATRA}). The value for deactivation rate constant (k_d) can then be calculated using $k_d = k_a/K_{ATRA}$. The activation rate constants in atom transfer radical processes (namely ATRA and ATRP) have been extensively examined in the literature and are typically determined from model studies in which the copper(I) complex is reacted with alkyl halide in the presence of radical trapping agents such as TEMPO (2,2,6,6-tetramethyl-1-piperidinyloxy) (Scheme 3).[43,61,68−70] Rates are determined

Scheme 3. Kinetic Isolation of the Activation Process in ATRA

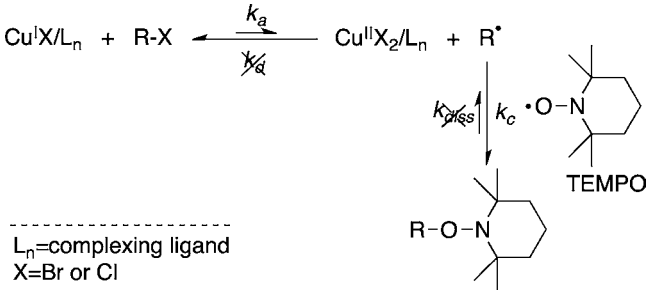

by monitoring the rate of disappearance of either alkyl halide or copper(I) complex in the presence of large excess of the second reagent (copper(I) complex or alkyl halide, respectively) and TEMPO. In the latter case, under such pseudo-first-order conditions, the activation rate constant can be calculated from $\ln([Cu^{I}]_o/[Cu^{I}]_t)$ versus t plots (slope = $k_a[RX]_o$).[71] The equilibrium constant for atom transfer (K_{ATRA}), on the other hand, is readily accessible from modified analytical solution of the persistent radical effect originally developed by Fischer and Fukuda.[58,59,66,72,73]

Copper complexes with TPMA ligand are among the most active catalysts for ATRA and ATRP reactions.[20,40,43] Recent study in our laboratory utilizing kinetic modeling indicated that the activation rate constants in the case of carbon tetrachloride and 2-chloro-2-methylpropanenitrile were on the order 1.0×10^5 M^{-1} s^{-1} at 60 °C.[21] Such fast rate constants are difficult to measure accurately using standard techniques such as NMR or UV−vis spectroscopy. Therefore, we decided to utilize pseudohalide benzyl thiocyanate, which is expected to significantly slow down the activation step. Benzyl thiocyanate (BzSCN) was synthesized by nucleophilic substitution of benzyl bromide with sodium thiocyanate, and the resulting product was confirmed as thiocyanate, as opposed to *iso*-thiocyanate, by NMR, IR, and single crystal X-ray diffraction (Figure 3a and Supporting Information). On the other hand,

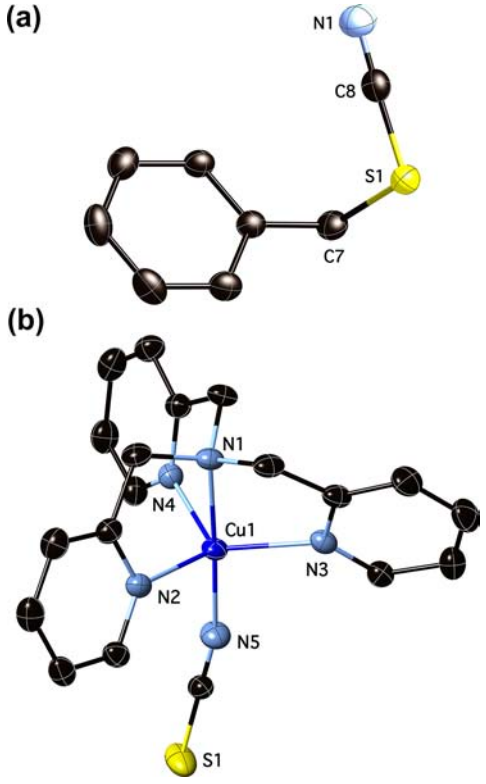

Figure 3. Molecular structures of benzyl thiocyanate (a) and $[Cu^{II}(TPMA)(NCS)][BPh_4]$ (b) at 150 K, shown with 50% probability displacement ellipsoids. H-atoms and counterion (BPh_4^-) have been omitted for clarity. Selected distances [Å] and angles [deg], benzyl thiocyanate: C7−S1 1.8492(18), S1−C8 1.6856(18), C8−N1 1.150(2), C7−S1−C8 98.91(8), S1−C8−N1 178.15(17). For $[Cu^{II}(TPMA)NCS][BPh_4]$: Cu1−N1 2.0194(11), Cu1−N2 2.0797(10), Cu1−N3 2.0569(11), Cu1−N4 2.0763(11), Cu1−N5 1.9189(12), N1−Cu1−N2 81.05(4), N1−Cu1−N3 81.45(4), N1−Cu1−N4 80.91(4), N1−Cu1−N5 177.84(5), N2−Cu1−N3 120.32(4), N3−Cu1−N4 119.51(4), N2−Cu1−N4 113.17(4), N5−Cu1−N2 97.26(5), N5−Cu1−N3 100.59(5), N5−Cu1−N4 98.60(5).

the molecular structure of $[Cu^{II}(TPMA)(NCS)][BPh_4]$ (Figure 3b), synthesized by either salt metathesis with NaSCN or oxidation of $Cu^{I}(TPMA)BPh_4$ with BzSCN, contained coordinated *iso*-thiocyanate anions. The results for K_{ATRA}, k_a, and k_d for BzSCN and $Cu^{I}(TPMA)Cl$ and $Cu^{I}(TPMA)BPh_4$ are summarized in Table 2. The equilibrium constant for atom transfer (K_{ATRA}) for tetraphenylborate complex ($(1.6 \pm 0.2) \times 10^{-7}$) was determined to be approximately 6 times larger than the chloride one ($(2.8 \pm 0.2) \times 10^{-8}$). This is in excellent agreement with the values for the apparent equilibrium constant (K_{ATRA}^{app}) determined from methyl acrylate ATRA kinetic data discussed above. What is even more important to notice is the fact that this difference was reflected in the activation rate constants ($(3.4 \pm 0.4) \times 10^{-4}$ M^{-1} s^{-1} (Cl^-) versus $(2.2 \pm 0.2) \times 10^{-3}$ M^{-1} s^{-1} (BPh_4^-)), indicating that both complexes have comparable deactivation capabilities ($(1.2 \pm 0.2) \times 10^4$ M^{-1} s^{-1} (Cl^-) versus $(1.4 \pm 0.5) \times 10^4$ M^{-1} s^{-1} (BPh_4^-)). Similar trends were observed previously for a series of copper complexes with neutral nitrogen based ligands and monohalogenated alkyl

dx.doi.org/10.1021/ic3018198 | *Inorg. Chem.* 2012, 51, 11917−11929

Table 2. Values of the Equilibrium Constant for Atom Transfer (K_{ATRA}), Activation (k_a), and Deactivation Rate Constants (k_d) for Benzyl Thiocyanate in CH_3CN at 23 ± 2 °C

complex	K_{ATRA}	k_a [M^{-1} s^{-1}]	k_d [M^{-1} s^{-1}][a]
Cu^I(TPMA)Cl	$(2.8 \pm 0.2) \times 10^{-8}$	$(3.4 \pm 0.4) \times 10^{-4}$	$(1.2 \pm 0.2) \times 10^{4}$
Cu^I(TPMA)BPh_4	$(1.6 \pm 0.2) \times 10^{-7}$	$(2.2 \pm 0.2) \times 10^{-3}$	$(1.4 \pm 0.5) \times 10^{4}$

[a]Calculated value ($k_d = k_a/K_{ATRA}$).

halides.[74] Furthermore, the experimentally determined activation rate constant for Cu^I(TPMA)Cl ($(3.4 \pm 0.4) \times 10^{-4}$ M^{-1} s^{-1}) is in excellent agreement with the predicted value (2.7×10^{-4} M^{-1} s^{-1}) obtained by extrapolation of kinetic data from other alkyl halides.[74,75]

The results discussed so far indicate that the activation rate constant in copper/TPMA catalyzed ATRA is dependent on the equilibrium constant for the coordination of the counterion to the $[Cu^I(TPMA)]^+$ cation and increases in the order Cl^- < ClO_4^- < BPh_4^-. Previously, we demonstrated that Cu^I(TPMA)Cl[16] and Cu^I(TPMA)Br[15] complexes contain coordinated halide anions in the solid state and are therefore saturated. If the same structures are present in solution, and since ATRA most likely involves an ISET (*vide supra*), the activation step with these catalysts must be preceded by ligand dissociation. We hypothesize that this could proceed along two different pathways: halide anion or partial TPMA dissociation, both of which could adequately explain the fluxionality of Cu^I(TPMA)Br or Cu^I(TPMA)Cl observed by variable temperature ^{1}H NMR (Scheme 4).[15,49] If the halide anion dissociates from the copper(I) center, the resulting $[Cu^I(TPMA)]^+$ cation can be stabilized by solvent or alkene (both of which are present in large excess)[46,63,64] and would act in a similar manner to complexes with less coordinating counterions (e.g., ClO_4^-, PF_6^-, or BPh_4^-). Alternatively, ligand arm dissociation from TPMA is also a possible route because it opens a coordination site for the incoming alkyl halide. In the latter case, the activation step does not necessarily require halide anion dissociation as depicted in Scheme 4. These two pathways are examined in the following sections of the Article.

Scheme 4. Possible Activation Pathways Involving Halide Anion or TPMA Arm Dissociation for Cu^I(TPMA)X (X = Br or Cl) Complexes

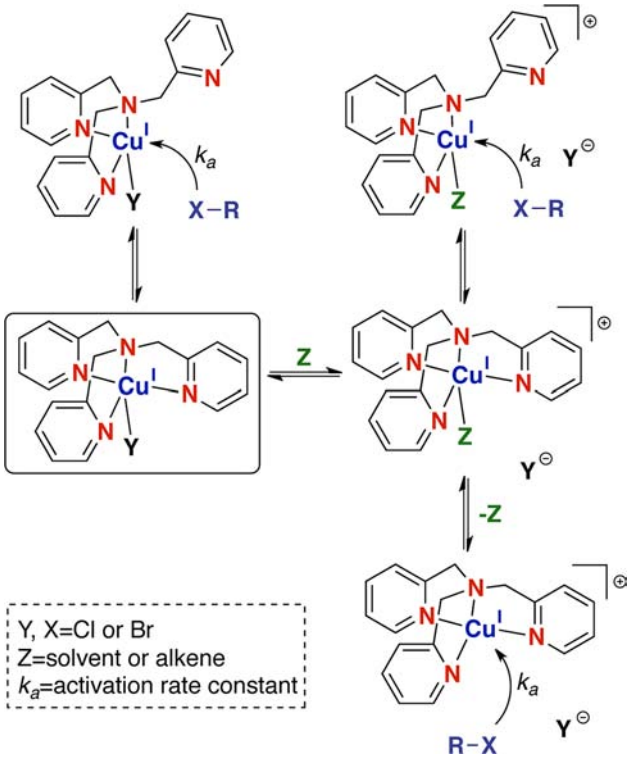

Halide Anion and TPMA Dissociation. The possibility of halide anion dissociation was examined first. Such dissociation, resulting in the formation of $[Cu^I(TPMA)(Z)]^+$ (Z = solvent or alkene) or even dimerized $[Cu_2^I(TPMA)_2]^{2+}$ species, could explain highly fluxional behavior of Cu^I(TPMA)X (X = Cl or Br) complexes observed by ^{1}H NMR spectroscopy at ambient temperatures.[15,49] If it indeed does occur in solution, the dissociation of halide anions from the copper(I) center could be suppressed by the addition of external source of halide anions. Shown in Figure 4 are ^{1}H NMR spectra of Cu^I(TPMA)Br complex in the presence of varying amounts of tetrabutylammonium bromide (TBA-Br). The addition of 1, 2, 5, and 10 equiv of TBA-Br does indeed sharpen the spectra significantly. However, as evident from Figure 4, the resulting spectra shift toward free TPMA indicating ligand displacement. Most likely, the presence of free bromide anions in the system shifts the equilibrium constant for the reaction $2Cu^I$(TPMA)Br → $[Cu^I(TPMA)][Cu^IBr_2]$ + TPMA toward its right-hand side. Also, there is a possibility for the formation of $[TBA][Cu^IBr_2]$, especially in the presence of large excess of TBABr. $[Cu^IBr_2]^-$ anions have been previously detected by extended X-ray

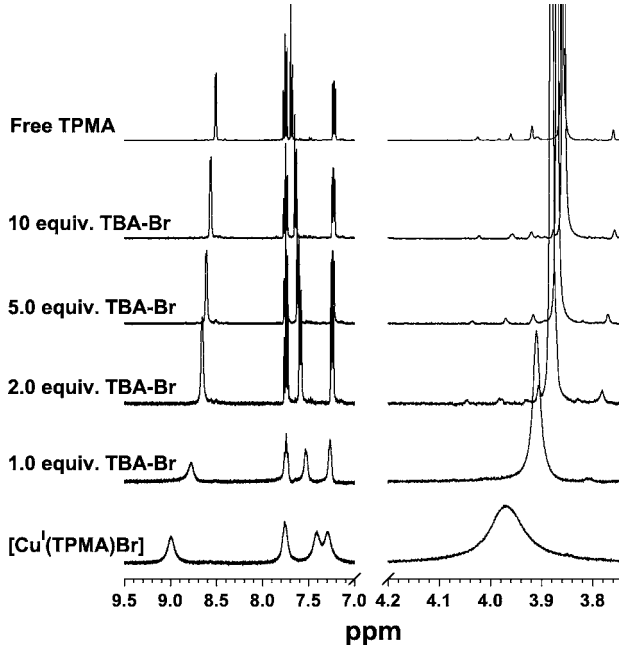

Figure 4. ^{1}H NMR (400 MHz, acetone-d_6, 298 K) spectra of Cu^I(TPMA)Br in the presence of tetrabutylammonium bromide (TBA-Br).

dx.doi.org/10.1021/ic3018198 | *Inorg. Chem.* 2012, 51, 11917–11929

absorption fine structure (EXAFS) spectroscopy in several ATRA/ATRP active catalytic systems.[76,77] They are generally rather inactive species in atom transfer radical processes. Indeed, when $[Cu^{II}(TPMA)X][X]$ (X = Cl or Br) catalyzed ATRA was carried out in the presence of AIBN and TBA-X (X = Cl or Br), a significant decrease in the yield of monoadduct was observed when more than 10 equiv of TBA-X were added relative to copper (see Supporting Information). Identical results were also observed with independently synthesized $[TBA][Cu^{I}X_2]$ (X = Cl or Br) complexes. This further illustrates the importance of TPMA ligand for activity of copper complexes in ATRA/ATRP.[78] Therefore, to the first approximation, it appears that the halide anion dissociation is not the primary cause for fluxionality observed in Cu^{I}(TPMA)-Br.

In order to further examine the position of the equilibrium between free versus coordinated halide anions in Cu^{I}/TPMA complexes, additional experiments were performed using cyclic voltammetry. As shown in Figure 5, nearly quantitative

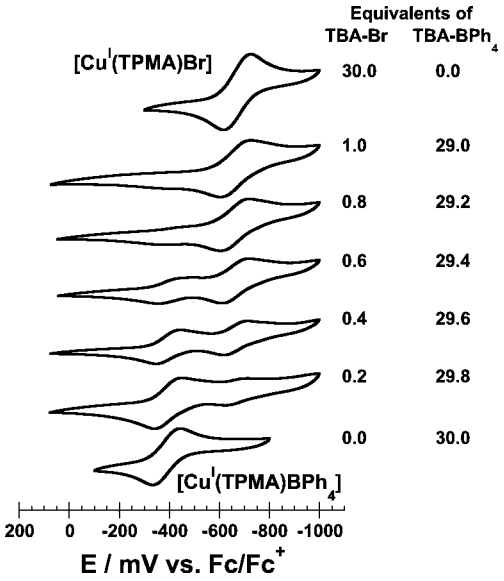

Figure 5. Cyclic voltammograms of $Cu^{I}(TPMA)BPh_4$ in the presence of TBA-Br and TBA-BPh_4 as supporting electrolytes (solvent = CH_3CN, scan rate = 100 mV/s, waves are reported with respect to Fc/Fc^+ couple).

conversion of $Cu^{I}(TPMA)BPh_4$ to Cu^{I}(TPMA)Br was observed with only a single equivalent of TBA-Br, clearly indicating the strong affinity of Br^- anions toward $[Cu^{I}(TPMA)]^+$ cations in solution. However, taking into account the sensitivity of cyclic voltammetry, solution conductivity measurements were also conducted. The results are summarized in Table 3. The conductivity of CH_3CN solutions of Cu^{I}(TPMA)Cl (2.64 μS/cm) and Cu^{I}(TPMA)Br (3.01 μS/cm) was found to be approximately half as large as for complexes with ClO_4^- (5.50 μS/cm) and BPh_4^- (6.29 μS/cm) counterions. This indicates that copper(I)/TPMA complexes with halide anions have less ionic character. However, the presence of conductivity in these complexes does suggest some degree of anion dissociation as well.

In Figure 5, it is also interesting to observe that copper(I)/TPMA complexes are much more reducing in the presence of halide anions than the less coordinating counterions such as ClO_4^-, BPh_4^-, or PF_6^-. A plausible explanation for the large

Table 3. Conductivity Values for $Cu^{I}(TPMA)Y$ (Y = Cl^-, Br^-, ClO_4^- and BPh_4^-) Complexes in CH_3CN at Ambient Temperature[a] (22 ± 3 °C)

complex	conductivity (μS/cm)
Cu^{I}(TPMA)Cl	2.64(±0.007)
Cu^{I}(TPMA)Br	3.01(±0.028)
$Cu^{I}(TPMA)ClO_4$	5.50(±0.064)
$Cu^{I}(TPMA)BPh_4$	6.29(±0.021)

[a]Determined in drybox (O_2 < 1.0 ppm), $[Cu^{I}]$ = 1.0 mM.

difference in redox potential lies in the stability of the corresponding copper(II) complex, which is generated by oxidation during electrochemical measurements. Recently reported log β values (β = stability constant, eq 5) for structurally related $[Cu^{II}(Me_6TREN)]^{2+}$ (27.2 ± 0.1) and $[Cu^{II}(Me_6TREN)Cl]^+$ (33.8 ± 0.1) complexes show that chloride anions have a much greater stabilizing effect for copper(II) species (Me_6TREN = tris(2-dimethylaminoethyl)-amine).[79−81] Since the redox potential is related to the relative stabilities of the Cu^{II} and Cu^{I} oxidation states (eq 6, L = complexing ligand),[46,47] the difference in RT/F $\ln(\beta^{II}/\beta^{I})$ values between $[Cu^{II}(Me_6TREN)]^{2+}$ and $[Cu^{II}(Me_6TREN)Cl]^+$ is nearly 270 mV (assuming $\beta^{I}([Cu^{I}(Me_6TREN)]^+)$ = $\beta^{I}(Cu^{I}(Me_6TREN)Cl) \approx 8.0 \times 10^{12}$).[80] Such a large difference in Cu^{II} stability constants is also the most likely reason for decreased redox potential observed for Cu^{I}/TPMA complexes with ClO_4^-, BPh_4^-, and PF_6^- anions.

$$\beta^m = \frac{[Cu^mL]}{[Cu^m][L]} \quad m = \text{I or II} \tag{5}$$

$$E \approx E^0 + \frac{RT}{F}\left(\ln \frac{[Cu^{II}]_{total}}{[Cu^{I}]_{total}} - \ln \frac{\beta^{II}}{\beta^{I}}\right) \tag{6}$$

So far, we were able to demonstrate that halide anions coordinate to $[Cu^{I}(TPMA)]^+$ cations in solution with a rather large equilibrium constant. Therefore, we reverted our attention to TPMA dissociation as the predominant reason for the fluxionality of Cu^{I}(TPMA)X (X = Cl or Br) complexes observed by ^{1}H NMR spectroscopy. Partial dissociation of TPMA is well documented in the solid state, particularly with bulky ligands such as PPh_3, or upon dimerization.[49,50,82] Hence, to confirm the fast ligand exchange on the NMR time scale, 1 equiv of free TPMA ligand was added to a solution of Cu^{I}(TPMA)Br in acetone-d_6. The representative ^{1}H NMR spectra are shown in Figure 6. At 280 K, five broad signals were observed, which were slightly sharpened when compared to previously reported Cu^{I}(TPMA)Br.[15] The signal for the pyridine protons (1), which is strongly shifted downfield as a result of coordination to the copper(I) center, was found to coalesce around 226 K. Below that temperature, the resonances for free and complexed TPMA were easily distinguishable (chemical shifts at 3.56 ppm (200 K) and 3.71 ppm (180 K) are from a solvent impurity). $\Delta H^{‡}$ and $\Delta S^{‡}$ for this exchange were determined from Erying plot and found to be 29.7 kJ mol^{-1} and −60.0 J K^{-1} mol^{-1}, respectively (see Supporting Information). Clearly, TPMA ligand in Cu^{I}(TPMA)Br complex is quite labile (e.g., $\Delta G^{‡}_{298}$ = 47.6 kJ $mol^{-1}$and $k_{obs,298} = 2.9 \times 10^4$ s^{-1}). These fast exchange rates also indicate that partial TPMA arm dissociation prior to the activation step in ATRA postulated in Scheme 4 indeed seems plausible, provided that ligand

dx.doi.org/10.1021/ic3018198 | Inorg. Chem. 2012, 51, 11917−11929

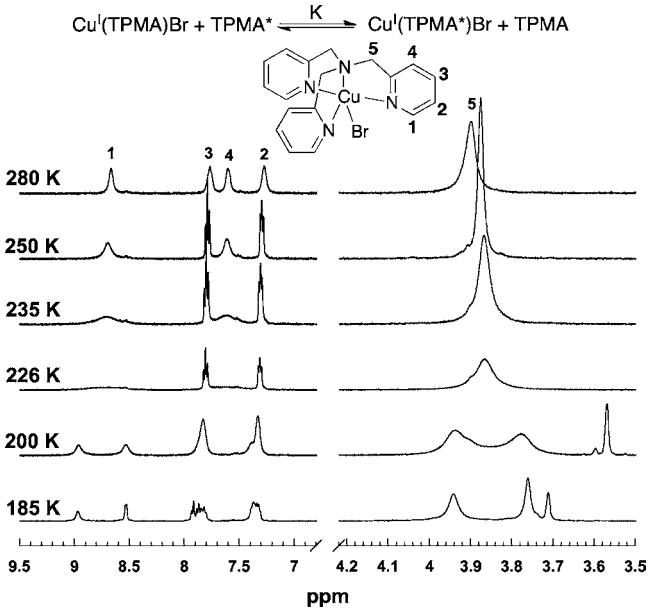

Figure 6. Variable temperature ^{1}H NMR (400 MHz, acetone-d_6) spectra of Cu^I(TPMA)Br in the presence of 1.0 equiv of TPMA ligand.

coordination/decoordination occurs through a stepwise process.

However, despite this fluxionality, it is again important to observe the significance of TPMA ligand for activity in copper catalyzed ATRA systems. Cu^{I}Br and Cu^{I}Cl salts at low concentrations used in this study were not found to produce monoadducts in quantities greater than those that can be attributed to free radical chain transfer initiated by AIBN (~20% with CCl_4 and 1-hexene). Furthermore, excess TPMA ligand was also added to ATRA reactions catalyzed by [Cu^{II}(TPMA)X][X] (X = Cl or Br) and was found to have no effect on alkene conversions or monoadduct yields in the presence of as many as 50 equiv relative to copper (see Supporting Information). Hence, from the thermodynamic point of view, TPMA dissociation from either Cu^I(TPMA)X or [Cu^{II}(TPMA)X][X] (X = Cl or Br) complexes is negligible. Indeed, recent measurements indicate that the equilibrium constants for binding of TPMA to copper complexes are rather large (~1.0×10^{12} for Cu^I and ~1.0×10^{17} for Cu^{II}).[80,83]

Triphenylphosphine Inhibition. In order to further examine the possibility for partial TPMA arm dissociation from the copper(I) center, additional ATRA experiments were performed in the presence of neutral triphenylphosphine. Previously, [Cu^I(TPMA)]$^+$ cations have been shown to accommodate such bulky ligand by dissociation of a single arm of TPMA, as demonstrated in the molecular structure of [Cu^I(TPMA)PPh_3][BPh_4] complex in the solid state.[50,82] The results for the addition of CCl_4 to various alkenes catalyzed by [Cu^{II}(TPMA)Cl][BPh_4] complex in the presence of PPh_3 and AIBN are summarized in Table 4. Interestingly, ATRA with 1-hexene and 1-octene catalyzed by 0.02 mol % of copper catalyst proceeded efficiently in the presence of as much as 10 equiv of free PPh_3. Further addition of the ligand resulted in a significant decrease in the yield of monoadduct for both alkenes. The same trend was also observed in the addition of CCl_4 to more active styrene and methyl acrylate catalyzed by 0.1 mol % of [Cu^{II}(TPMA)Cl][BPh_4]. For both alkenes, relative low yields in the absence of PPh_3 can be attributed to inefficient radical trapping after the first addition step or free radical polymerization initiated by AIBN. Kinetic experiments were also performed in order to examine the effect of PPh_3 on the conversion of alkene. The representative plots in the case of 1-octene are shown in Figure 7. The observed rates also mimic the trend found in the yield of monoadduct and decrease nearly 7 times in the presence of 0 ($k_{obs} = 1.5 \times 10^{-5}$ s^{-1}) and 20 ($k_{obs} = 2.3 \times 10^{-6}$ s^{-1}) equiv of PPh_3, respectively. However, what is even more important to notice is the fact that the rates remain nearly constant in the range 0−5 equiv of free ligand. Under such reaction conditions, it is reasonable to assume that the predominant activator species in the solution generated by the reduction of [Cu^{II}(TPMA)Cl][BPh_4] are [Cu^I(TPMA′)PPh_3]-[BPh_4] (TPMA′ denotes partially decoordinated TPMA ligand). The fact that the activity of [Cu^I(TPMA′)PPh_3][BPh_4] ($k_{obs} = 1.5 \times 10^{-5}$ s^{-1}) and Cu^I(TPMA)BPh_4 ($k_{obs} = 1.4 \times 10^{-5}$ s^{-1}) in the addition of CCl_4 to 1-octene is nearly identical strongly supports the hypothesis that the activation step in ATRA can occur after partial dissociation of one of the arms in TPMA ligand. At elevated concentrations of PPh_3 (10−20 equiv relative to copper), the formation of well-known and documented [Cu(PPh_3)$_x$][A] (A = counterion, x = 3 or 4) is

Table 4. ATRA of CCl_4 to Different Alkenes Catalyzed by [Cu^{II}(TPMA)Cl][BPh_4] in the Presence of PPh_3 and AIBN[a]

		equiv of PPh_3				
alkene	$[Alk]_0:[Cu^{II}]_0$	0[b]	2	10	20	40
1-hexene	5000:1	~100	~100	~100	84	38
1-octene	5000:1	~100	~100	~100	71	22
styrene	1000:1	31	24	0	0	0
methyl acrylate	1000:1	50	49	38	35	0

[a]All reactions were performed in CH_3CN at 60 °C with $[CCl_4]_0/[alkene]_0/[AIBN]_0 = 1/1/0.05$, $[alkene]_0 = 2.40$ M. The yield is based on the formation of monoadduct after 24 h and was determined by ^{1}H NMR spectroscopy using 1,4-dimethoxybenzene as an internal standard (relative errors are ±5.0%). [b]Molar equivalents of PPh_3 relative to copper catalyst.

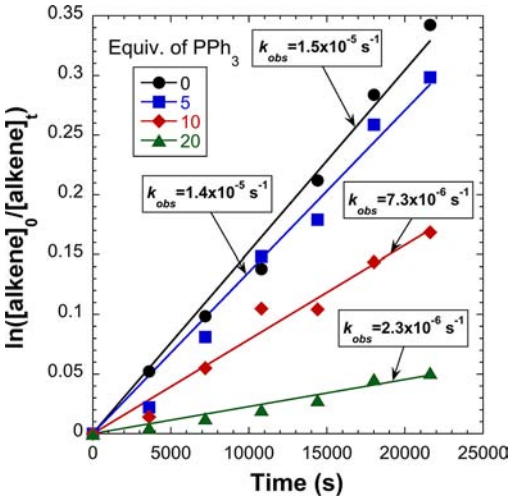

Figure 7. First order kinetic plots for ATRA of CCl_4 and 1-octene catalyzed by [Cu^{II}(TPMA)Cl][BPh_4] in the presence of 0, 5, 10, and 20 equiv of free PPh_3 (relative to catalyst). Reactions were performed at 60 °C in CH_3CN, $[1\text{-alkene}]_0/[CCl_4]_0/[AIBN]_0/[Cu]_0 = 500/500/25/1$, $[alkene]_0 = 2.40$ M. Conversions were determined by ^{1}H NMR spectroscopy using 1,4-dimethoxybenzene as an internal standard (relative errors are ±15%).

dx.doi.org/10.1021/ic3018198 | Inorg. Chem. 2012, 51, 11917−11929

quite likely. Complexes of this type, namely $[Cu^{I}(PPh_3)_3(CH_3CN)][ClO_4]$, $[Cu^{I}(PPh_3)_3][BPh_4]$, and $[Cu^{I}(PPh_3)_3(PPh_3')][BPh_4]$ (PPh_3' denotes partially coordinated PPh_3 ligand (Cu–P = 3.9551(17) Å)) were independently synthesized according to modified literature procedures[84−87] and were found to have no activity in ATRA. Some representative structures are shown in the Supporting Information. Thus, a decrease in the alkene conversion (Figure 7) and the yield of monoadduct (Table 4) in the presence of large excess of triphenylphosphine is expected, as observed experimentally.

ATRA with Tris(2-(dimethylamino)phenyl)amine (TDAPA) Ligand. In order to further confirm that coordinatively saturated copper(I)/TPMA complexes can participate in the activation step during ATRA by opening the coordination site via arm dissociation, we sought to prepare a structurally similar ligand that would have reduced arm mobility. Neutral tetradentate tris(2-(dimethylamino)phenyl)-amine (TDAPA)[52] was an ideal candidate because is it a structural "hybrid" between TPMA and Me_6TREN, which are currently among the most active ligands for copper catalyzed ATRA (Scheme 5).[43,76] Indeed, the molecular structure of

Scheme 5. Structural Similarities between TDAPA and TPMA/Me_6TREN Ligands

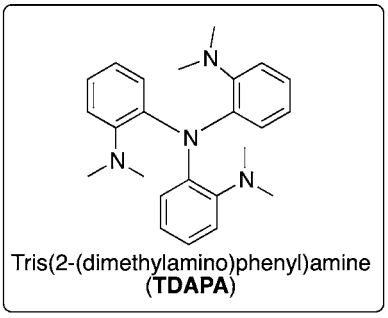

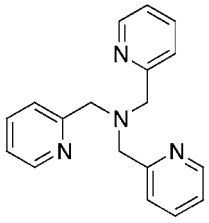
Tris(2-pyridylmethyl)amine
(TPMA)

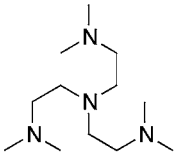
Tris(2-(dimethylamino)ethyl)amine
(Me_6TREN)

$[Cu^{I}(TDAPA)(CH_3CN)][ClO_4]$ (Figure 8) showed many similarities to previously reported $[Cu^{I}(TPMA)(CH_3CN)][BPh_4]$ complex.[50] The copper(I) center in $[Cu^{I}(TDAPA)(CH_3CN)][ClO_4]$ was pseudo-pentacoordinated in the solid state due to the coordination of the axial nitrogen atom from TDAPA (2.372(2) Å). Furthermore, the equatorial Cu^{I}–N bond lengths (2.234(2), 2.267(3), and 2.206 (2) Å) were nearly equal and slightly longer than observed in $[Cu^{I}(TPMA)(CH_3CN)][BPh_4]$ (~2.100 Å). Ignoring the axial coordination of the nitrogen atom from TDAPA, all other angles around copper(I) center were close to that of a regular tetrahedron. On the other hand, previously reported copper(II) complexes with TDAPA ligand were found to adopt a trigonal bipyramidal geometry similar to the one observed with TPMA and Me_6TREN ligands.[52] However, despite these structural

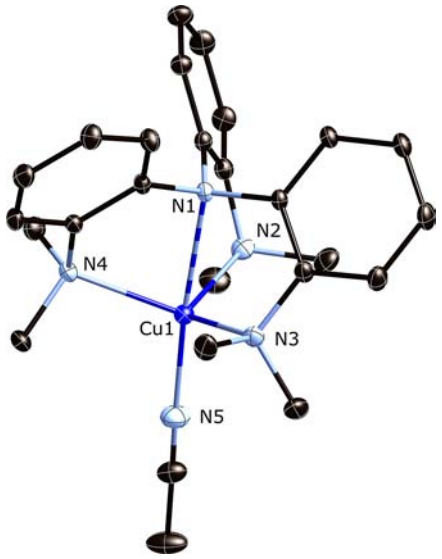

Figure 8. Molecular structure of $[Cu^{I}(TDAPA)(CH_3CN)][ClO_4]$ at 150 K, shown with 30% probability displacement ellipsoids. H-atoms and counterion have been omitted for clarity. Selected bond distances [Å] and angles [deg]: Cu1–N1 2.372(2), Cu1–N2 2.234(2), Cu1–N3 2.267(3), Cu1–N4 2.206(2), Cu1–N5 1.953(3), N1–Cu1–N2 75.69(8), N1–Cu1–N3 75.03(8), N1–Cu1–N4 75.77(8), N1–Cu1–N5 175.49(11), N2–Cu1–N3 115.86(9), N2–Cu1–N4 113.40(9), N3–Cu1–N4 112.57(9), N2–Cu1–N5 103.09(12), N3–Cu1–N5 101.90(12), N4–Cu1–N5 108.60(11).

similarities, it is apparent from Figure 8 that TDAPA backbone is quite rigid. The main reasons are the restrictions in the ligand arm mobility due to not only the steric effects, but also the lack of free rotation around sp^2 hybridized atoms of the phenyl rings adjacent to the two coordinating nitrogen atoms. Therefore, we suspected that the activation step in ATRA with TDAPA ligand as a result of arm dissociation would be slower when compared to TPMA complexes. The results for the addition of CCl_4 to various alkenes catalyzed by $[Cu^{II}(TDAPA)Cl][A]$ (A = Cl^-, BF_4^-, and BPh_4^-) complexes in the presence of AIBN are summarized in Table 5.

As evident from Table 5, very poor activity of $[Cu^{II}(TDAPA)Cl][Cl]$ was observed in the addition of CCl_4

Table 5. ATRA of CCl_4 to Different Alkenes Catalyzed by $[Cu^{II}(TDAPA)Cl][Y]$ (Y = Cl^-, BF_4^-, and BPh_4^-) in the Presence of AIBN[a]

alkene	anion	conversion (%)	yield (%)
1-hexene	Cl^-	24	24
1-octene		25	25
styrene		41	7
methyl acrylate		100	1
1-hexene	BF_4^-	49	49
1-octene		59	59
styrene		50	35
methyl acrylate		100	10
1-hexene	BPh_4^-	60	60
1-octene		45	45

[a]All reactions were performed at 60 °C in CH_3CN with $[alkene]_0/[CCl_4]_0/[AIBN]_0/[Cu]_0$ = 250/250/12.5/1, $[alkene]_0$ = 2.40 M. The yield is based on the formation of monoadduct after 24 h and was determined by ^1H NMR spectroscopy using 1,4-dimethoxybenzene as an internal standard (relative errors are ±5.0%).

dx.doi.org/10.1021/ic3018198 | Inorg. Chem. 2012, 51, 11917−11929

to 1-hexene, 1-octene, styrene, and methyl acrylate. The addition of CCl_4 to 1-hexene and 1-octene resulted in mere 25% yields of the monoadduct using catalyst loading as high as 0.4 mol %. With $[Cu^{II}(TPMA)Cl][Cl]$, nearly quantitative yields of the desired product were obtained at catalyst loadings as low as 0.02 mol %.[16] The results for styrene and methyl acrylate were even more detrimental, and the high conversions for both monomers can only be attributed to free radical polymerization initiated by radicals generated from thermal decomposition of AIBN. As a matter of fact, the ATRA results with $[Cu^{II}(TDAPA)Cl][Cl]$ were not significantly better than those achieved in the absence of catalyst via conventional Kharasch addition, suggesting that these complexes are completely inactive in ATRA. We believe that the activator in this system is coordinatively saturated $Cu^{I}(TDAPA)Cl$. If the chloride anion is tightly bound to the copper(I) center, this complex is limited in starting the ATRA cycle by homolytically cleaving the carbon−halogen bond in CCl_4, since the arm mobility is restricted by the rigid ligand backbone. These results are very significant from the point of view of TPMA discussed throughout this Article because they demonstrate that coordinatively saturated $Cu^{I}(TPMA)X$ (X = Cl or Br) complexes can participate in the activation step in ATRA via ligand arm dissociation.

Taking into account the results discussed above, the only remaining possibility to increase the activity of $Cu^{I}(TDAPA)Cl$ complex in ATRA is to replace the bound halide anion with less coordinating counterion. Indeed, as indicated in Table 5, $Cu^{I}(TDAPA)BF_4$ and $Cu^{I}(TDAPA)BPh_4$ complexes showed improved activity in monoadduct yields for both 1-hexene and 1-octene (45−60%) under identical reaction conditions. Therefore, it is clear that, in the case of neutral tetradentate nitrogen based ligands, halide anion and arm dissociation play an important role in the activation step in ATRA.

CONCLUSIONS

In summary, kinetic and mechanistic studies of atom transfer radical addition (ATRA) catalyzed by copper complexes with tris(2-pyridylmethyl)amine (TPMA) ligand were reported. In solution, the halide anions were found to strongly coordinate to $[Cu^{I}(TPMA)]^+$ cations, as confirmed by kinetic, cyclic voltammetry, and conductivity measurements. $Cu^{I}(TPMA)X$ (X = Cl or Br) complexes were found to be more reducing than the corresponding ones containing less coordinating counterions (PF_6^-, ClO_4^-, and BPh_4^-), which was attributed to much higher complex stability of the corresponding $[Cu^{II}(TPMA)X]^+$ species. Furthermore, the equilibrium constant for atom transfer (K_{ATRA}) utilizing benzyl thiocyanate was determined to be approximately six times larger for $Cu^{I}(TPMA)BPh_4$ ($(1.6 \pm 0.2) \times 10^{-7}$) than $Cu^{I}(TPMA)Cl$ ($(2.8 \pm 0.2) \times 10^{-8}$) complex. These results were in excellent agreement with the values for the apparent equilibrium constant (K_{ATRA}^{app}) determined from ATRA kinetic data. Interestingly, this difference in reactivity between $Cu^{I}(TPMA)Cl$ and $Cu^{I}(TPMA)BPh_4$ complexes was reflected in the activation rate constants ($(3.4 \pm 0.4) \times 10^{-4}$ M^{-1} s^{-1} and $(2.2 \pm 0.2) \times 10^{-3}$ M^{-1} s^{-1}, respectively), indicating that both complexes have comparable deactivation capabilities ($(1.2 \pm 0.2) \times 10^{4}$ M^{-1} s^{-1} and $(1.4 \pm 0.5) \times 10^{4}$ M^{-1} s^{-1}, respectively). The fluxionality of $Cu^{I}(TPMA)X$ in solution was mainly the result of TPMA ligand exchange, which for the bromide complex was found to be very fast at ambient temperature ($\Delta H^{\ddagger}$ = 29.7 kJ mol^{-1}, $\Delta S^{\ddagger}$ = −60.0 J K^{-1} mol^{-1}, $\Delta G^{\ddagger}_{298}$ = 47.6 kJ mol^{-1}, and $k_{obs,298} = 2.9 \times 10^{4}$ s^{-1}). Relatively strong coordination of halide anions in $Cu^{I}(TPMA)X$ prompted the possibility of activation in ATRA through partial TPMA dissociation. Indeed, no visible differences in the ATRA activity of $Cu^{I}(TPMA)BPh_4$ were observed in the presence of as many as 5 equiv of strongly coordinating triphenylphosphine. Under such reaction conditions, the predominant activator species in the solution were $[Cu^{I}(TPMA')PPh_3][BPh_4]$ (TPMA′ denotes a tricoordinated TPMA). The possibility for arm dissociation in $Cu^{I}(TPMA)X$ was further confirmed by synthesizing tris(2-(dimethylamino)-phenyl)amine (TDAPA), a ligand that was structurally similar to currently most active TPMA and Me_6TREN (tris(2-dimethylaminoethyl)amine), but had a limited arm mobility due to the rigid backbone. Indeed, $Cu^{I}(TDAPA)Cl$ complex was found to be inactive in ATRA, and the activity increased only by opening the coordination site around copper(I) center by replacing chloride anion with less coordinating counterions such as BF_4^- and BPh_4^-. The results presented in this Article are significant from the mechanistic point of view because they indicate that coordinatively saturated $Cu^{I}(TPMA)X$ complexes catalyze the homolytic cleavage of carbon−halogen bond during the activation step in ATRA by prior dissociation of either halide anion or TPMA arm.

ASSOCIATED CONTENT

Supporting Information

Crystal tables, kinetic plots for the determination of the equilibrium constant for atom transfer (K_{ATRA}) and activation rate constant (k_a), and ^{1}H NMR and infrared spectra. Crystallographic data in CIF format. This material is available free of charge via the Internet at http://pubs.acs.org.

AUTHOR INFORMATION

Corresponding Author

*E-mail: pintauert@duq.edu. Phone: 412-396-1626. Fax: 412-396-5683.

Notes

The authors declare no competing financial interest.

ACKNOWLEDGMENTS

Financial support from National Science Foundation Career Award (CHE-0844131) is gratefully acknowledged. Authors also thank Prof. Cora MacBeth and Nicole Ando from Emory University for providing TDAPA ligand and William Brennessel from the University of Rochester for his help in final stages of single crystal X-ray refinements.

REFERENCES

(1) Kharasch, M. S.; Jensen, E. V.; Urry, W. H. *J. Am. Chem. Soc.* **1946**, *68*, 154−155.
(2) Kharasch, M. S.; Jensen, E. V.; Urry, W. H. *Science* **1945**, *102*, 128.
(3) Severin, K. *Curr. Org. Chem.* **2006**, *10*, 217−224.
(4) Quebatte, L.; Scopelliti, R.; Severin, K. *Eur. J. Inorg. Chem.* **2005**, 3353−3358.
(5) Quebatte, L.; Haas, M.; Solari, E.; Scopelliti, R.; Nguyen, Q. T.; Severin, K. *Angew. Chem., Int. Ed.* **2004**, *43*, 1520−1524.
(6) Clark, A. J. *Chem. Soc. Rev.* **2002**, *31*, 1−11.
(7) Clark, A. J.; Dell, C. P.; Ellard, J. M.; Hunt, N. A.; McDonagh, J. P. *Tetrahedron Lett.* **1999**, *40*, 8619−8623.
(8) Bland, W. J.; Davis, R.; Durrant, J.; Jim, L. A. *J. Organomet. Chem.* **1984**, *267*, C45−C48.
(9) Nagashima, H.; Wakamatsu, H.; Itoh, K.; Tomo, Y.; Tsuji, J. *Tetrahedron Lett.* **1983**, *24*, 2395−2398.

(10) Minisci, F. *Acc. Chem. Res.* **1975**, *8*, 165−171.
(11) Asscher, M.; Vosfsi, D. *J. Chem. Soc.* **1963**, 1887−1896.
(12) Asscher, M.; Vosfsi, D. *J. Chem. Soc.* **1963**, 3921−3927.
(13) Pintauer, T. *ACS Symp. Ser.* **2009**, *1023*, 63−84.
(14) Eckenhoff, W. T.; Pintauer, T. *Catal. Rev.: Sci. Eng.* **2009**, *51*, 1−59.
(15) Eckenhoff, W. T.; Garrity, S. T.; Pintauer, T. *Eur. J. Inorg. Chem.* **2008**, 563−571.
(16) Eckenhoff, W. T.; Pintauer, T. *Inorg. Chem.* **2007**, *46*, 5844−5846.
(17) Quebatte, L.; Thommes, K.; Severin, K. *J. Am. Chem. Soc.* **2006**, *128*, 7440−7441.
(18) Nair, R. P.; Kim, T. H.; Frost, B. J. *Organometallics* **2009**, *28*, 4681−4688.
(19) Lundgren, R. J.; Rankin, M. A.; McDonald, R.; Stradiotto, M. *Organometallics* **2008**, *27*, 254−258.
(20) Pintauer, T. *Eur. J. Inorg. Chem.* **2010**, *17*, 2449−2460.
(21) Balili, M. N. C.; Pintauer, T. *Inorg. Chem.* **2010**, *49*, 5642−5649.
(22) Ricardo, C. L.; Pintauer, T. *Chem. Commun.* **2009**, 3029−3031.
(23) Balili, M. N. C.; Pintauer, T. *Inorg. Chem.* **2009**, *48*, 9018−9026.
(24) Ricardo, C. L.; Pintauer, T. *Eur. J. Inorg. Chem.* **2011**, 1292−1301.
(25) Eckenhoff, W. T.; Pintauer, T. *Dalton Trans.* **2011**, *40*, 4909−4917.
(26) Balili, M. N. C.; Pintauer, T. *Dalton Trans.* **2011**, *40*, 3060−3066.
(27) Eckenhoff, W. T.; Biernesser, A. B.; Pintauer, T. *Inorg. Chim. Acta* **2012**, *382*, 84−95.
(28) Pintauer, T.; Eckenhoff, W. T.; Ricardo, C. L.; Balili, M. N. C.; Biernesser, A. B.; Noonan, S. T.; Taylor, M. J. W. *Chem.—Eur. J.* **2009**, *15*, 38−41.
(29) Thommes, K.; Severin, K. *Chimia* **2010**, *64*, 188−190.
(30) Wolf, J.; Thommes, K.; Briel, O.; Scopelliti, R.; Severin, K. *Organometallics* **2008**, *27*, 4464−4474.
(31) Muñoz-Molina, J. M.; Belderrain, T. R.; Pérez, P. J. *Adv. Synth. Catal.* **2008**, *350*, 2365−2372.
(32) Fernández-Zúmel, M. A.; Kiefer, G.; Thommes, K.; Scopelliti, R.; Severin, K. *Eur. J. Inorg. Chem.* **2010**, 3596−3601.
(33) Thommes, K.; Kiefer, G.; Scopelliti, R.; Severin, K. *Angew. Chem., Int. Ed.* **2009**, *48*, 8115−8119.
(34) Fernandez-Zumel, M. A.; Thommes, K.; Kiefer, G.; Sienkiewicz, A.; Pierzchala, K.; Severin, K. *Chem.—Eur. J.* **2009**, *15*, 11601−11607.
(35) Thommes, K.; Icli, B.; Scopelliti, R.; Severin, K. *Chem.—Eur. J.* **2007**, *13*, 6899−6907.
(36) Thommes, K.; Fernández-Zúmel, M. A.; Buron, C.; Godinat, A.; Scopelliti, R.; Severin, K. *Eur. J. Org. Chem.* **2011**, 249−255.
(37) Taylor, M. J. W.; Eckenhoff, W. T.; Pintauer, T. *Dalton Trans.* **2010**, *39*, 11475−11482.
(38) Eckenhoff, W. T.; Pintauer, T. *Cat. Rev.: Sci. Eng.* **2010**, *51*, 1−59.
(39) Muñoz-Molina, J. M.; Belderrain, T. R.; Pérez, P. J. *Eur. J. Inorg. Chem.* **2011**, 3155−3164.
(40) Pintauer, T.; Matyjaszewski, K. *Chem. Soc. Rev.* **2008**, *37*, 1087−1097.
(41) Curran, D. P. *Synthesis* **1988**, 489−513.
(42) Odian, G. *Principles of Polymerization*, 4th ed.; John Wiley & Sons: Hoboken, NJ, 2004.
(43) Pintauer, T.; Matyjaszewski, K. *Top. Organomet. Chem.* **2009**, *26*, 221−251.
(44) Matyjaszewski, K. *Macromolecules* **1998**, *31*, 4710−4717.
(45) Matyjaszewski, K.; Xia, J. *Chem. Rev.* **2001**, *101*, 2921−2990.
(46) Tsarevsky, N.; Braunecker, W. A.; Vacca, A.; Gans, P.; Matyjaszewski, K. *Macromol. Symp.* **2007**, *248*, 60−70.
(47) Tsarevsky, N.; Braunecker, W. A.; Matyjaszewski, K. *J. Organomet. Chem.* **2007**, *692*, 3212−3222.
(48) Lin, C. Y.; Coote, M. L.; Gennaro, A.; Matyjaszewski, K. *J. Am. Chem. Soc.* **2008**, *130*, 12762−12774.
(49) Hsu, S. C.; Chien, S. S.; Chen, H. H.; Chiang, M. Y. *J. Chin. Chem. Soc.* **2007**, *54*, 685−692.
(50) Eckenhoff, W. T.; Pintauer, T. *Inorg. Chem.* **2010**, *49*, 10617−10626.
(51) Britovsek, G.; England, J.; White, A. *Inorg. Chem.* **2005**, *44*, 8125−8134.
(52) Chu, L.; Hardcastle, K. I.; MacBeth, C. E. *Inorg. Chem.* **2010**, *49*, 7521−7529.
(53) Munakata, M.; Kitagawa, S.; Asahara, A.; Masuda, H. *Bull. Chem. Soc. Jpn.* **1987**, *60*, 1927−1929.
(54) Sheldrick, G. M. *SADABS Version 2.03*; University of Gottingen: Gottingen, Germany, 2002.
(55) Sheldrick, G. M. *SHELXTL 6.1,Crystallographic Computing System*; Bruker Analytical X-Ray System: Madison, WI, 2000.
(56) Faruggia, L. J. *J. Appl. Crystallogr.* **1997**, *30* (5, Pt. 1), 565.
(57) Crabtree, R. H. In *The Organometallic Chemistry of the Transition Metals*, 4th ed.; John Wiley & Sons Inc.: Hoboken, NJ, 2005; pp 275−296.
(58) Fischer, H. *Chem. Rev.* **2001**, *101*, 3581−3610.
(59) Tang, W.; Tsarevsky, N. V.; Matyjaszewski, K. *J. Am. Chem. Soc.* **2006**, *128*, 1598−1604.
(60) Pintauer, T.; Zhou, P.; Matyjaszewski, K. *J. Am. Chem. Soc.* **2002**, *124*, 8196−8197.
(61) Matyjaszewski, K.; Paik, H.; Zhou, P.; Diamanti, S. J. *Macromolecules* **2001**, *34*, 5125−5131.
(62) Qiu, J.; Matyjaszewski, K.; Thouin, L.; Amatore, C. *Macromol. Chem. Phys.* **2000**, *201*, 1625−1631.
(63) Braunecker, W.; Pintauer, T.; Tsarevsky, N.; Kickelbick, G.; Matyjaszewski, K. *J. Organomet. Chem.* **2005**, *690*, 916−924.
(64) Braunecker, W. A.; Tsarevsky, N. V.; Pintauer, T.; Gil, R. R.; Matyjaszewski, K. *Macromolecules* **2005**, *38*, 4081−4088.
(65) Matyjaszewski, K.; Jakubowski, W.; Min, K.; Tang, W.; Huang, J.; Braunecker, W. A.; Tsarevsky, N. V. *Proc. Nat. Acad. Sci.* **2006**, *103*, 15309−15314.
(66) Fischer, H. *J. Am. Chem. Soc.* **1986**, *108*, 3925−3927.
(67) Fischer, H. *J. Polym. Sci., Part A: Polym. Chem.* **1999**, *37*, 1885−1901.
(68) Goto, A.; Fukuda, T. *Macromol. Rapid Commun.* **1999**, *20*, 633−636.
(69) Ohno, K.; Goto, A.; Fukuda, T.; Xia, J.; Matyjaszewski, K. *Macromolecules* **1998**, *31*, 2699−2701.
(70) Pintauer, T.; Zhou, P.; Matyjaszewski, K. *J. Am. Chem. Soc.* **2002**, *124*, 8196−8197.
(71) Pintauer, T.; Braunecker, W. A.; Collange, E.; Poli, R.; Matyjaszewski, K. *Macromolecules* **2004**, *37*, 2679−2682.
(72) Fischer, H. *J. Polym. Sci., Part A: Polym. Chem.* **1999**, *37*, 1885−1901.
(73) Goto, A.; Fukuda, T. *Prog. Polym. Sci.* **2004**, *29*, 329−385.
(74) Tang, W.; Kwak, Y.; Braunecker, W.; Tsarevsky, N. V.; Coote, M. L.; Matyjaszewski, K. *J. Am. Chem. Soc.* **2008**, *130*, 10702−10713.
(75) Tang, W.; Matyjaszewski, K. *Macromolecules* **2007**, *40*, 1858−1863.
(76) Pintauer, T.; Matyjaszewski, K. *Coord. Chem. Rev.* **2005**, *249*, 1155−1184.
(77) Pintauer, T.; Reinohl, U.; Feth, M.; Bertagnolli, H.; Matyjaszewski, K. *Eur. J. Inorg. Chem.* **2003**, 2082−2094.
(78) Borguet, Y. P.; Tsarevsky, N. V. T. *Polym. Chem.* **2012**, *3*, 2487−2494.
(79) Bortolamei, N.; Isse, A. A.; Di Marco, V. B.; Gennaro, A.; Matyjaszewski, K. *Macromolecules* **2010**, *43*, 9257−9267.
(80) Ambundo, E. A.; Deydier, M. V.; Grall, A. J.; Aguera-Vega, N.; Dressel, L. T.; Cooper, T. H.; Heeg, M. J.; Ochrymowycz, L. A.; Rorabacher, D. B. *Inorg. Chem.* **1999**, *38*, 4233−4242.
(81) Golub, G.; Lashaz, A.; Cohen, A.; Paoletti, P.; Bencini, A.; Valtancoli, B.; Meyerstein, D. *Inorg. Chim. Acta* **1997**, *255*, 111−115.
(82) Tyeklar, Z.; Jacobson, R. R.; Wei, N.; Murthy, N. N.; Zubieta, J.; Karlin, K. D. *J. Am. Chem. Soc.* **1993**, *115*, 2677−2689.
(83) Braunecker, W.; Matyjaszewski, K. *Prog. Polym. Sci.* **2007**, *32*, 93−146.
(84) Barron, P. F.; Dyason, J. C.; Engelhardt, L. M.; Healy, P. C.; White, A. H. *Aust. J. Chem.* **1985**, *38*, 261−271.

(85) Hanna, J. V.; Boyd, S. E.; Healy, P. C.; Bowmaker, G. A.; Skeltond, B. W.; White, A. H. *J. Chem. Soc., Dalton Trans.* **2005**, *1*, 2547−2556.
(86) Healy, P. C.; Hanna, J. V. *Acta Crystallogr., Sect. E.* **2003**, *E59*, m384−m386.
(87) Gaughan, A. P.; Dori, Z.; Ibers, J. A. *Inorg. Chem.* **1974**, *13*, 1657−1667.